THE JOURNAL OF PHYSICAL CHEMISTRY B

Article

Use of Picosecond Fluorescence Dynamics as an Indicator of Exciton Motion in Conjugated Polymers: Dependence on Chemical Structure and Temperature

Thomas G. Bjorklund, Sang-Hyun Lim, and Christopher J. Bardeen

J. Phys. Chem. B, **2001**, 105 (48), 11970-11977 • DOI: 10.1021/jp0124746

Use of Picosecond Fluorescence Dynamics as an Indicator of Exciton Motion in Conjugated Polymers: Dependence on Chemical Structure and Temperature

Thomas G. Bjorklund, Sang-Hyun Lim, and Christopher J. Bardeen*

Department of Chemistry, University of Illinois, 600 S. Mathews Ave., Urbana, Illinois 61801

Received: June 29, 2001; In Final Form: September 18, 2001

The utility of picosecond fluorescence dynamics as an experimental indicator of exciton motion in conjugated polymers is assessed by examining the fluorescence dynamics of phenylene vinylene polymers and oligomers as a function of temperature and chemical derivatization. Both polycrystalline poly(*p*-phenylene vinylene) (PPV) and an oligomeric analogue in polystyrene exhibit similar picosecond fluorescence Stokes shifts at all temperatures, indicating that this shift is due mostly to intramolecular relaxation. In PPV, the decay time of the integrated fluorescence decreases from 800 ps at 16 K (close to the oligomer lifetime of 930 ps) to 200 ps at 290 K and is accompanied by an increase in the anisotropy decay. A simple model for the dependence of the fluorescence decay on the exciton diffusion yields an activation energy of 170 cm^{-1} for exciton motion in PPV. In contrast to the unsubstituted PPV, poly[(2-methoxy-5-hexyloxy-*p*-phenylene)vinylene] (MH−PPV) forms an amorphous solid whose fluorescence Stokes shift is twice that observed for isolated MH−PPV molecules dissolved in a poly(vinyl chloride) (PVC) host polymer. The increased Stokes shift and spectral changes in MH−PPV provide evidence for excimer formation which is absent in PPV. The 250 ps decay of the integrated fluorescence in MH−PPV exhibits almost no temperature dependence and is considerably faster than the decay rate of the isolated polymer in PVC. The differences between PPV and MH−PPV are rationalized based on differences in the solid-state intermolecular interactions. This work shows how the excited-state emission dynamics in these materials may be due to local phenomena like intramolecular vibrational relaxation (PPV) or excimer formation (MH−PPV) as opposed to exciton diffusion.

I. Introduction

The optical and electronic properties of conjugated electroluminescent organic polymers have made them attractive candidates for applications in light emitting diodes and solar cells. Despite the fact that their charge mobilities are often orders of magnitude smaller than those found in inorganic semiconductors, it has been possible to incorporate these materials into high efficiency light emitting diodes.[1] In these materials, the luminescent species is a Frenkel exciton, formed when an electron/hole pair recombines, which is extends over 7−15 repeat units of the polymer.[2] The electroluminescence efficiency is tied to the dynamics of the exciton, resulting in an active effort to characterize exciton behavior in these materials. The study of exciton dynamics in conjugated polymers is simplified by the fact that in many cases their photoluminescence and electroluminescence spectra are identical, meaning that one can directly create the exciton species of interest through photoexcitation as well as charge recombination. Thus, the standard methods of optical spectroscopy may be used to interrogate exciton structure and dynamics.

It is thought that the exciton dynamics in conjugated polymers are strongly influenced by excited state electronic energy transfer among the densely packed chromophores. From a practical standpoint, exciton migration to quenching defects increases the nonradiative decay rate and lowers the luminescence efficiency of a light emitting diode. Exciton diffusion has been inferred from bulk spectroscopic measurements of the time-dependent shifting of the emission to lower energies,[3,4] presumably due to exciton migration to lower energy sites,[5] and the depolarization of the emission.[6] Microscopic measurements of the radius of photobleaching[7] or the spatial emission profile[8] after excitation using a near-field scanning optical microscope tip, as well as single molecule studies,[9] have also provided evidence of exciton migration in these materials. It is important to determine whether these methods accurately reflect exciton motion in order to know whether certain assumptions concerning the relation between molecular-level sample morphology and luminescence efficiency are correct. For instance, high crystallinity leads to high charge carrier mobilities and thus a higher yield of electron−hole pairs which form excitons but may also enhance exciton mobility, making it easier for those excitons to move around and find quenching defects before they fluoresce. Adding side chains to a polymer can increase the disorder and lower exciton mobility, improving the luminescence yield once an exciton is formed, but it also makes it more difficult for charges to move around and form the luminescent exciton in the first place. Finding the correct balance between these approaches requires a consistent measure of exciton mobility in these materials.

As mentioned above, time-dependent fluorescence has been used as a tool to monitor energy transfer in conjugated systems by many workers, both through energy shifting and depolarization. In this paper, we examine the time-dependent luminescence of two phenylene vinylene polymers in order to determine whether this measurement provides insight into exciton motion and to sort out the effects of chemical structure on the dynamics of fluorescence and energy transfer. The first polymer, poly-

* To whom correspondence should be addressed. Fax: 1-217-244-3186. E-mail: bardeen@scs.uiuc.edu.

10.1021/jp0124746 CCC: $20.00
Published on Web 11/01/2001

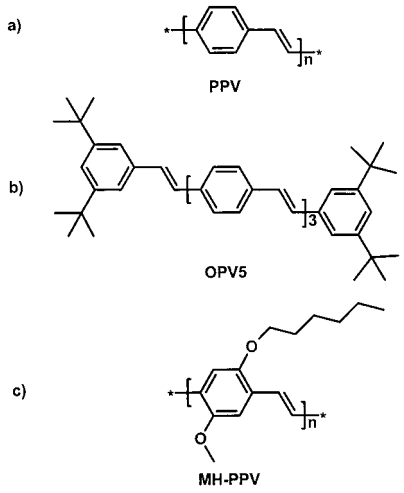

Figure 1. Molecular structures of (a) PPV, (b) OPV5, and (c) MH−PPV.

(*p*-phenylene vinylene) (PPV), whose structure is shown in Figure 1a, is formed by thermal conversion of a precursor, resulting in an insoluble, polycrystalline solid. We compare its dynamics with those of the oligomer shown in Figure 1b, which contains five phenyl groups and approaches the degree of conjugation observed in PPV. The dynamic Stokes shifts of these two systems are identical at all temperatures, suggesting that this observable is not a reliable indicator of exciton motion. By analyzing the temperature-dependent fluorescence decay and anisotropy, we find that the energy transfer dynamics in PPV can be understood in terms of activated hopping from site to site, similar to that observed in molecular crystals. We compare the dynamics in PPV to those of a PPV derivative, poly[(2-methoxy-5-hexyloxy-*p*-phenylene)vinylene] (MH−PPV), where the phenyl group now has alkoxy side chains added to increase solubility and decrease crystallinity. This polymer, which is very similar to the widely studied poly[(2-methoxy-5-(2′-ethylhexyloxy)-*p*-phenylene)vinylene] (MEH−PPV) in terms of its room-temperature absorption and emission spectra and its fluorescence decay, shows different behavior from PPV. Neat MH−PPV exhibits a larger Stokes shift than isolated MH−PPV molecules dissolved in a poly(vinyl chloride) host polymer, but this is due largely to the formation of a long-lived, strongly redshifted species, probably an excimer, which is absent in PPV. The 250 ps fluorescence decay in MH−PPV has almost no temperature dependence and is considerably faster than the decay rate observed for isolated MH−PPV molecules.

Our work leads to two main conclusions. First, caution must be used when inferring exciton motion from dynamic Stokes shift data: for PPV, the origin of the Stokes shift appears to be mainly intramolecular in origin, whereas in MH−PPV, it reflects rapid excimer formation. In neither case is there a clear relation between the wavelength dependence of the dynamics and exciton diffusion. Second, the information contained in the fluorescence dynamics depends on the detailed chemical structure of the polymer. As expected, the more crystalline PPV has more pronounced exciton diffusion, but this is inferred from the temperature-dependent fluorescence and anisotropy decays. Although the side chains on MH−PPV prevent the formation of the crystalline domains observed in unsubstituted PPV, thus suppressing exciton diffusion, they appear to enhance excimer formation, leading to a fast, temperature-independent decay channel.

II. Experimental Section

The PPV film samples were prepared from a precursor polymer with a tetrahydrothiophenium leaving group.[10−12] Equal amounts of a 0.4 M aqueous solution of *p*-xylylenebis-(tetrahydrothiophenium chloride) and a 0.4 M NaOH solution were reacted under an argon atmosphere with stirring at 0 °C. The reaction was stopped after two minutes and thirty seconds by adding a 0.6 M HCl solution. The polymer solution was transparent, viscous and had a final pH between 2 and 3. The solution was transferred to regenerated cellulose dialysis tubing (Fisher, 3500 MWCO) and dialyzed against water for 48 h changing the water every 12 h. The precursor solution was used right out of the tubing without further processing and stored in a sealed container inside a refrigerator.[12,13] This differs from the more common method of making PPV precursor where the water is removed through dialysis and the polymer redissolved in methanol for spin casting.[11] We have found that the water solutions lead to more ordered films with a more resolved absorption spectrum, although the transient behavior remains the same.[14] The precursor solutions can be stored for at least one month in a freezer or refrigerator without any detectable sign of degradation in the absorption.[15] Precursor samples were spin cast on 12.5 mm diameter 0.5 mm thick sapphire substrates at 600 rpm to make films that were approximately 50 nm in thickness as measured using a Dektak profilometer. The spun precursor films were converted under vacuum (<30 mTorr) at 300 °C for 3 h in a tube furnace. The converted films were transferred to a cryostat under an argon atmosphere and stored under vacuum in the cryostat. The converted PPV films were characterized with UV/vis absorption and infrared absorption. The typical optical density of sample films was 0.5−0.7 at the peak of the visible absorption spectrum. Infrared absorption spectra of thicker films showed no discernible carbonyl peak around 1600 cm^{-1}, implying oxidation of these samples was negligible.

Poly[(2-methoxy-5-hexyloxy-*p*-phenylene)vinylene] (MH−PPV) was synthesized using a Gilch-polymerization procedure adapted from Burn et al.[16] 1,4-bis(chloromethyl)-2-hexyloxy-5-methoxybenzene was reacted in THF with excess potassium *tert*-butoxide for 12 h producing a red-orange color solution of MH−PPV. This solution was then concentrated and precipitated into methanol and filtered to produce a dark-red solid polymer. This polymer was stored in a sealed container in a dark freezer until use. MH−PPV films were spun from THF solutions onto 12.5 mm diameter 0.5 mm thick sapphire substrates. Blends were made with poly(vinyl chloride) in THF and either drop cast or spin cast onto sapphire as well. Both types of sample were made with optical densities of 0.3 or more at 500 nm.

The *tert*-butyl substituted oligomer was synthesized using a procedure developed by Müllen and co-workers.[17] The 3,5-di-*tert*-butyltoluene was functionalized and repeat units attached through successive Wittig reactions. When the desired length is reached, two chains are joined through a Wittig reaction with terephthaldicarboxaldehyde. The oligomer containing five phenyl rings (OPV5) was then mixed with polystyrene in methylene chloride to make a 10^{-6} M solution of oligomer in polystyrene. The oligomer/polymer blend was then drop cast to make a good optical quality film with an absorption of 0.3 at 400 nm.

X-ray diffraction spectra of the unoriented PPV and MH−PPV samples were measured over a 2θ range of 0−60° using a Bruker AXS rotating anode monochromator as the source of Cu Kα radiation (λ = 1.54 Å) for a Bruker AXS P4 single-crystal X-ray diffractometer with a Bruker AXS HI−STAR area detector. The crystallite sizes in the PPV films were calculated

from the X-ray diffraction pattern using the Scherrer equation (eq 1):[18]

$$D_{hkl} = \frac{K\lambda}{\beta_{1/2} \cos \theta} \quad (1)$$

Using this equation, the true peak widths of the sample ($\beta_{1/2}$), the wavelength of the X-ray radiation (λ), the detection angle (θ), and a shape parameter (K), the average dimension of the crystallites along the axis normal to the plane can be calculated. To get the true peak widths of the sample, the instrument broadening had to be measured and then deconvoluted from the measured peaks. A lanthanum hexaboride standard (NIST SRM 660a) was used to measure the instrument broadening. The half widths of the peaks were then used to obtain the dimensions.

Picosecond time-resolved fluorescence measurements were taken using a streak camera (Hamamatsu, streak scope C4334). The samples were held under vacuum in the cold head of a compressed helium cryostat where the temperatures were varied from 16 to 290 K. The 400 nm excitation pulses were made by second harmonic generation of the 800 nm output of a 40 kHz regenerative amplifier (Spectra Physics, Spitfire) in a 0.4 mm BBO with a pulse width of about 200 fs. The 500 nm excitation pulses were generated using a home-built noncollinear optical parametric amplifier pumped with the same 40 kHz amplifier.[19,20] Samples were excited with the beam coming in at an angle of about 20° from the sample surface normal. For lifetime measurements, the sample was excited at the magic angle (54.7°) relative to the detection polarization to minimize depolarization effects. For the anisotropy measurements, a polarizer in the pump beam was rotated to provide excitation polarized either parallel or perpendicular to the detection polarizer. The fluorescence was collected normal to the sample surface, collimated, and focused into a 0.150 m path length spectrometer (Spectra Pro-150) with a 150 grooves/mm grating giving us a spectral detection window of about 190 nm with the streak camera and a resolution of 3 nm. The full-width at half-maximum for the instrument response for the 5 ns sweep window used in these experiments is 50−70 ps. Excitation powers were less than 1 μW with a focal spot of about 50 μm in diameter, resulting in a maximum excitation density of 2.7×10^{17} cm^{-3}. This is well below the threshold for amplified spontaneous emission or exciton−exciton annihilation.[21,22]

III. Results

Figure 2a shows the room-temperature absorption and emission spectra for neat PPV and the OPV5 oligomer dissolved in polystyrene. Both molecules have structured spectra, a result of the C−C double bond vibration in the range from 1300 to 1500 cm^{-1} found in PPVs and other conjugated systems.[23] As the sample is cooled, both the absorption and emission spectra in PPV become more resolved and shift to lower energy, and the shape of the fluorescence changes in a way consistent with a decrease in the Huang−Rhys parameter due to increasing conjugation as low-frequency torsional modes are frozen out.[24−26] These changes are not observed in the oligomer spectra, which are independent of temperature. MH−PPV has a broad featureless absorption that peaks at 520 nm and an emission spectrum that shows a high-frequency vibronic progression similar to that observed in PPV. There is little difference between the spectra of neat MH−PPV and dilute MH−PPV in a PVC host, and for both, the emission spectrum shows only slight sharpening as the temperature drops and no dramatic shift in vibronic oscillator strength as observed for PPV.

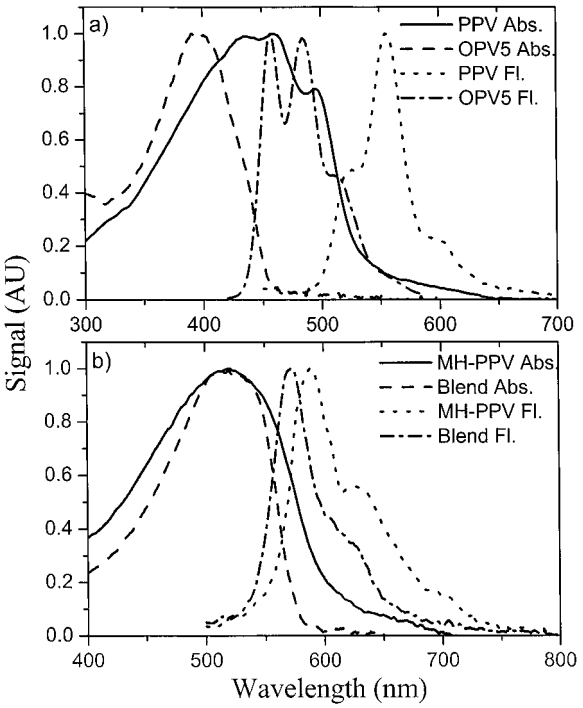

Figure 2. (a) Room-temperature absorption and fluorescence spectra of PPV (—, absorption; − − −, fluorescence] and OPV5 (− −, absorption; − - −, fluorescence). (b) Room-temperature absorption and fluorescence spectra of neat MH−PPV (—, absorption; − − − fluorescence) and the MH−PPV/PVC blend (− −, absorption; − - −, fluorescence). The vibronic structure seen in the PPV absorption and all of the emission spectra correspond to the 1300−1500 cm^{-1} C−C double bond vibration of PPVs.

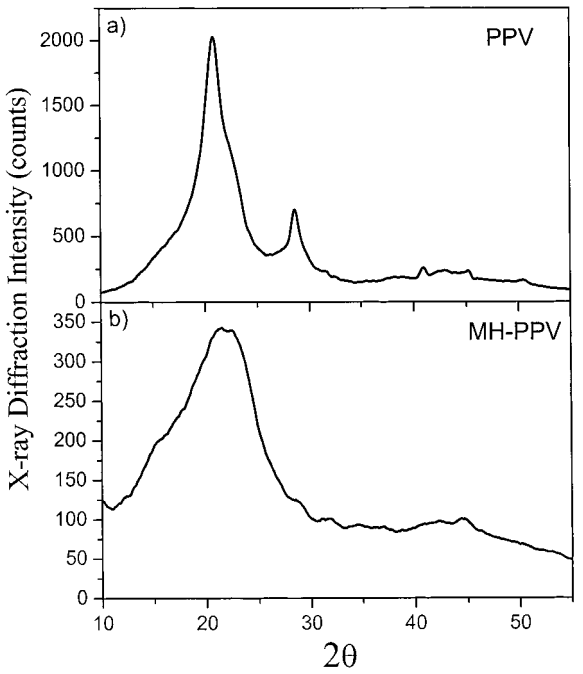

Figure 3. X-ray diffraction profiles for (a) PPV and (b) MH−PPV. PPV has a discernible intermolecular lattice spacing peak at 20° (110) with a shoulder (200) and another at 28° (210). MH−PPV has no discernible peaks corresponding to intermolecular lattice spacings.

Room-temperature X-ray diffraction profiles of PPV and MH−PPV are shown in Figure 3. MH−PPV has a single broad peak on top of a large amorphous background, with no discernible peaks corresponding to intermolecular crystal planes. The PPV profile also has an amorphous background, but it is

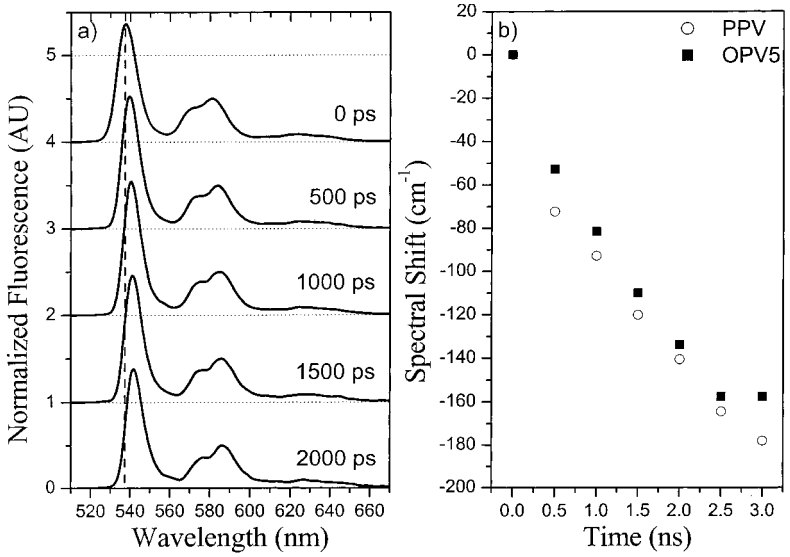

Figure 4. (a) Time-resolved fluorescence spectrum of PPV at 16 K over the first 2000 ps after excitation at 400 nm. The shape of the spectrum does not change over the first 2000 ps. The dashed vertical line indicates the 0−0 peak at 0 ps. (b) The Stokes shift of the 0−0 peak in cm^{-1} at 16 K over the first 3 ns after excitation for PPV and OPV5. The PPV shift, 180 cm^{-1}, is nearly the same as OPV5, 160 cm^{-1}.

smaller and there is considerable diffraction intensity in two distinct peaks at 20° and 28°. These peaks correspond, respectively, to the (110) and (210) planes observed previously for oriented PPV samples that were identified as having a p2gg unit cell.[27,28] This "herringbone" motif is common in unsubstituted poly-acene systems such as anthracene and sexithiophene.[29,30] From the widths of the resolved diffraction peaks in PPV, we estimate the average crystal size to be approximately 5 nm in the 110 direction and 10 nm in the 210 direction, both of which are perpendicular to the long axis of the PPV chain. These dimensions are consistent with direct measurements using dark field TEM.[31] Assuming the crystallite dimensions above and approximating the crystallite shape to be roughly rectangular along the unit cell axes in the plane perpendicular to the chain axis, there are 60 unit cells in the average crystallite domain. This indicates that these domains contain on the order of 120 PPV molecules. Because MH−PPV has no discernible single peaks and crystallite size is inversely proportional to peak width, it is reasonable to assume from our data that any kind of crystallite in MH−PPV is very small and the sample is essentially amorphous.

Having characterized the static properties of our samples, we turn to the fluorescence dynamics. The time evolution of the PPV emission spectra at 16 K is shown in Figure 4a. We will refer to the first two peaks as 0−0 and 0−1 for both the PPV and MH−PPV spectra. The 0−0 peak is the highest energy peak in the spectrum, and the 0−1 peak is the next highest in energy. Note that the spectrum at low temperature has a different shape from the room-temperature spectrum shown in Figure 2 due to the freezing out of the torsional modes and increased conjugation.[24−26] PPVs emission spectra show both the 0−0 and 0−1 peaks having the same decay times with the spectral shape changing very little over the first 2000 ps after excitation. Much of the spectral shifting and reshaping in PPV at this temperature actually occurs at delays below the time resolution of this measurement and have been observed through femtosecond pump−probe and upconversion experiments.[3,4,25] From Figure 4b, which plots the frequency shift of the 0−0 peaks at 16 K, we see that PPV and its oligomer have almost identical Stokes shifts of 180 and 160 cm^{-1}, respectively. As the temperature increases, the emission peaks broaden and the shifts decrease, until at room temperature their shifts are <30 cm^{-1} over 3 ns. The spectral shifting of neat PPV and dilute OPV5 in PS are similar at all temperatures and neither sample shows evidence of spectral reshaping on this time scale.

The fluorescence dynamics in MH−PPV at 16 K are shown in Figure 5a. At this temperature, a comparison of the wavelength shifting in MH−PPV and its blend show they are not as similar as PPV and OPV5. The neat polymer shows a much greater fluorescence redshift, 350 cm^{-1}, than the dilute blend, 130 cm^{-1}. Most of this shift occurs within the first nanosecond after excitation. The emission spectrum of neat MH−PPV also shows a change in shape, with the 0−0 peak of the spectrum decaying faster than the 0−1 peak. Although the shape of the PPV fluorescence is constant over the first 2 ns, the MH−PPV spectrum changes from a well-resolved vibronic progression, with the 0−0 peak roughly twice the height of the 0−1 peak, to a broad almost shapeless spectrum where the two peaks are barely discernible. The MH−PPV/PVC blend, by comparison, shows a total shift of 130 cm^{-1}, similar to that of PPV and OPV5, and no changes in spectral shape. As the temperature increases, the peaks broaden and the total Stokes shift decreases for both the neat polymer and the blend, but even at room temperature, the neat polymer still shows a greater redshift, 170 cm^{-1}, as opposed to less than 30 cm^{-1} for the blend.

Integrating the wavelength-resolved data from Figures 4 and 5, we obtain decay curves for the integrated fluorescence. Measurement of the decay at a fixed wavelength does not necessarily reflect the total excited-state population at a given instant in time because of the shifting of the fluorescence through a specific wavelength window.[25] Figure 6a shows the decay of the integrated fluorescence for PPV at 16, 100, and 290 K, along with the decay of OPV5 in polystyrene at 16 K. Although the fluorescence decay times in PPV show a strong temperature dependence, slowing by a factor of 4 at low temperature, the oligomer decay is independent of temperature. Unlike OPV5, the PPV decays are not single exponentials. More complex models from the literature using parameters describing the diffusion of excitons to traps do a reasonable job of fitting the first two nanoseconds of the decay but still cannot accurately fit the long time portion of the decay data.[32−38] This long time data is most likely due to slow recombination of free charges created by the initial excitation pulse.[37] For this reason, we have

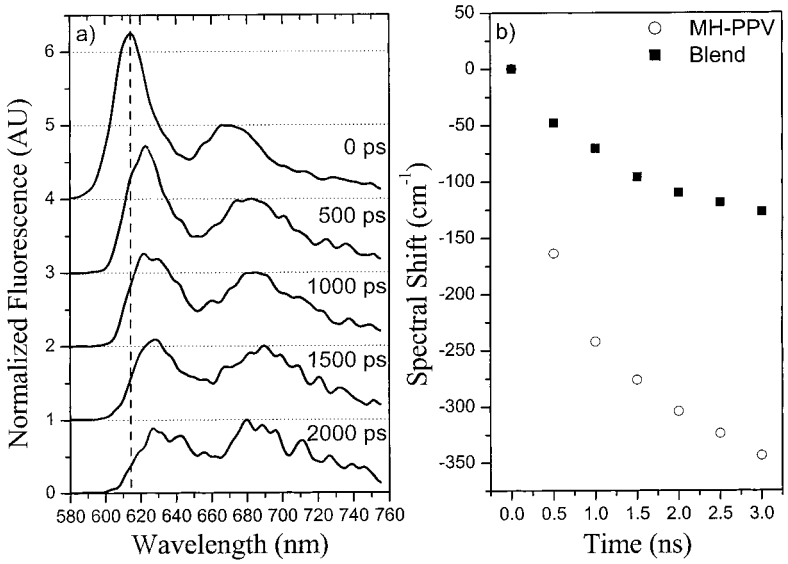

Figure 5. (a) Time-resolved fluorescence spectrum of MH−PPV at 16 K over the first 2000 ps after excitation at 500 nm. The spectral shape changes in the first 2000 ps with 0−0 peak quickly decaying, and the entire spectrum becomes a single broad redshifted feature. The dashed vertical line indicates the 0−0 peak at 0 ps. (b) The 0−0 Stokes shift in cm^{-1} at 16 K over the first 3 ns after excitation for MH−PPV and MH−PPV/PVC blend.

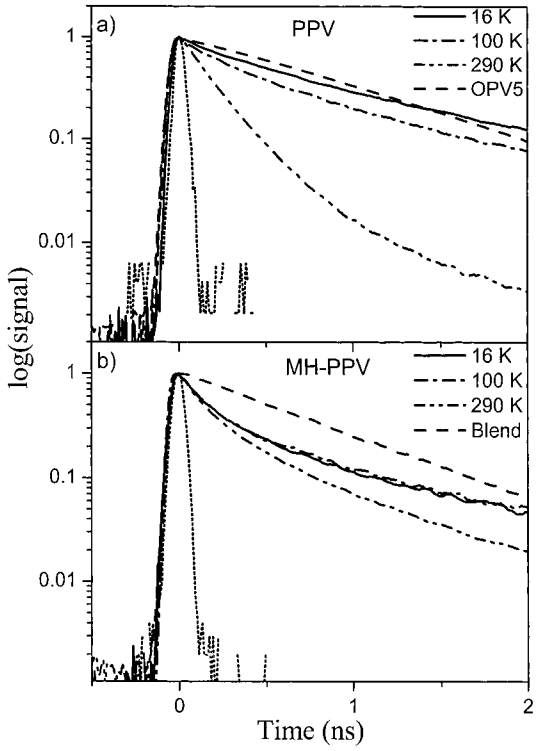

Figure 6. (a) Temperature dependence of the fluorescence decays for neat PPV at 16 (—), 100 (– - –), and 290 K (– - - –), along with the fluorescence decay of OPV5/PS at 16 K (– –). (b) Fluorescence decays of neat MH−PPV and the MH−PPV/PVC blend under the same conditions as PPV in part a. PPV shows a strong temperature dependence with the decays getting faster with temperature, whereas MH−PPV has almost no temperature dependence. Both neat polymer films exhibit nonexponential fluorescence decays at long times.

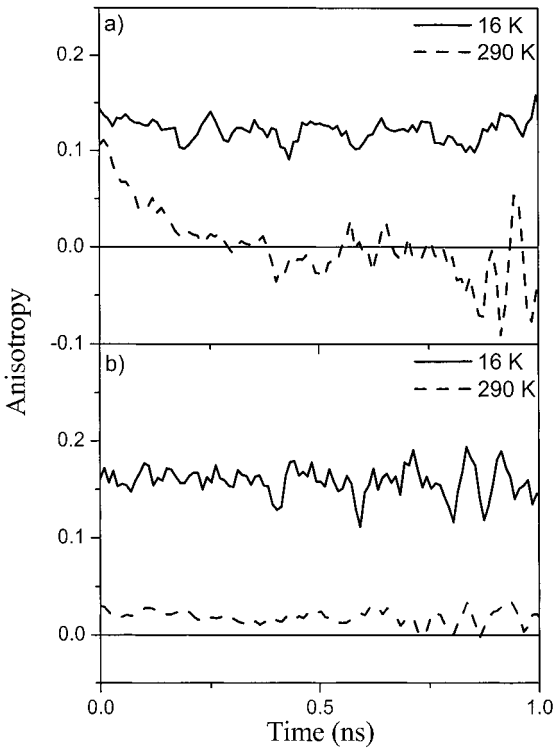

Figure 7. Temperature dependence of anisotropy signal at 16 (—) and 290 K (– –) for (a) PPV and (b) MH−PPV. The anisotropy of PPV is constant at 16 K but decays at 290 K due to exciton diffusion. MH−PPV has a constant anisotropy at both 16 and 290 K, but its magnitude drops from 0.15 to 0.025 as the temperature is increased from 16 to 290 K.

limited our fits to the first nanosecond of the decays that we describe as an exponential decay (eq 2) with competing radiative and nonradiative processes having rates k_r and k_{nr}, respectively:

$$y = A^* \exp[(-k_r + k_{nr})t] \qquad (2)$$

This is equivalent to assuming simple Smoluchowski diffusion to quenching sites which neglects the effects of fluctuations in trap density[32] and short-time decay due to excitons created adjacent to trap sites.[39] The assumption that k_{nr} is the result of exciton diffusion to trapping sites is supported by our time-resolved anisotropy data, shown in Figure 7, which measures the randomization of the fluorescence transition dipoles as a function of time. The increase in PPVs fluorescence decay rate is accompanied by an increased anisotropy decay rate (Figure 7a), which is absent in the OPV5 data. Measurements at 16 K

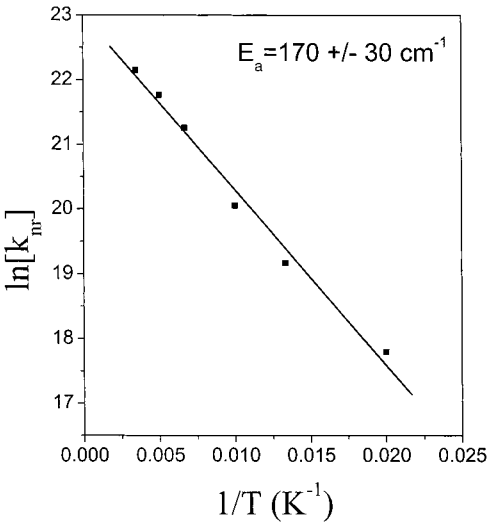

Figure 8. Arrhenius plot of temperature-dependent early-time (1 ns) PPV fluorescence decay rates. The slope corresponds to an activation energy (E_a) of 170 ± 30 cm^{-1} for the nonradiative process.

show a constant anisotropy in the range of 0.1−0.2. Increasing the temperature shows the anisotropies start to decay toward zero, and at 290 K the anisotropy decays to zero in about 400 ps. We set k_r to 1.2 ns for all temperatures[40,41] and allow only k_{nr} to vary in our exponential fits of the early time data. Using the measured rates and temperatures we then make an Arrhenius plot (Figure 8) and obtain an activation energy for the nonradiative process k_{nr} of 170 ± 30 cm^{-1}. Using more complicated models for the fluorescence decay lead to similar activation energies in the range of 150 −200 cm^{-1}. Although the absolute rate k_{nr} will depend on details of sample preparation, such as trap density, this affects only the Arrhenius prefactor and not the activation energy obtained for energy transport.

The temperature dependence of MH−PPVs fluorescence decay is much weaker than that of PPV, as can be seen in Figure 6b. A slight increase in the decay rate at room temperature was insufficient to allow an accurate estimation of the activation energy for this material, because any change with temperature is close to the experimental noise. Also shown for comparison is the MH−PPV blend with PVC, whose decay remains constant over the temperature range from 16 to 290 K. Comparing MH−PPV to a dilute blend of MH−PPV/PVC shows that the isolated molecules have a longer decay time suggesting the presence of a nonradiative process in the neat film that is relatively insensitive to temperature. Similar to PPV, the fluorescence decay of the MH−PPV films is nonexponential and probably represents the effects of several processes, including charge recombination. The anisotropy of MH−PPV (Figure 7b) is constant at 16 K with a value of about 0.15 and also constant at 290 K with a value of about 0.02.

IV. Discussion

The predominant thought on PPV dynamics is that upon excitation the excitons formed quickly diffuse to luminescence quenching sites causing a fast initial fluorescence decay followed by a slower recombination process resulting in a long luminescent tail.[37] The focus of this discussion will be on the former process and examine the time range from about 100 ps to 2 ns. Our data show that, at low temperatures, both PPV and MH−PPV exhibit large fluorescence Stokes shifts within the first 2 ns after photoexcitation. Although such shifting suggests the possibility that we are directly observing exciton migration through a manifold of energies to low energy sites,[5] our data does not support this scenario. Our measurements show that the Stokes shift for PPV and OPV5 over the first 2 ns after excitation is the same (Figure 4b) within experimental error. Given the fact that the concentration of OPV5 in polystyrene was 10^{-6} M, the intermolecular spacing would be about 120 nm. This spacing between the OPV5 molecules is too large for Förster energy transfer processes. Hence, the Stokes shift observed in OPV5 must be due to intramolecular relaxation processes. Assuming the same intramolecular processes also occur in PPV, the majority of the dynamic Stokes shifting in PPV is also likely to be intramolecular in origin, suggesting that the luminescence shifting is not a good indicator of intermolecular energy transfer in PPV.

Although the spectral shifting in PPV contains no information about exciton diffusion, its temperature-dependent fluorescence decays do provide evidence for such diffusion.[42] The data in Figure 6a show a factor of 4 decrease in decay time from 800 to 200 ps when increasing the temperature from 16 to 290 K, whereas the decay time for the OPV5 sample is 930 ps at all temperatures. From the PPV data, we were able to extract an activation energy for the energy hopping of 170 ± 30 cm^{-1}. Interestingly, this activation energy results in a turning on of the diffusion in the temperature range between 100 and 200 K, which is also where the steady-state emission spectrum is observed to change shape.[25,26] This suggests that the two processes may be controlled by molecular motions in the same energy range, which in this case correspond to low-frequency ring torsions of the polymer.[43,44] The fluorescence spectra are consistent with the temperature decrease freezing out ring torsions which in turn increases the average conjugation length of chain segments in the polymer. This also explains the temperature dependence of the Stokes shift: as the temperature is increased, the thermal energy in the low-frequency coordinate becomes comparable to the relaxation energy, which leads to a broadening and blueshift of the steady-state spectrum and less discernible shifting in the transient spectrum. These same torsions may also result in fluctuations in the $\pi-\pi$ interactions between molecules and aid in the diffusion of excitons from site to site until it is quenched by some defect.[41,45] Freezing out these torsions lowers the probability of site-to-site transfer until the radiative decay becomes the dominant process for exciton relaxation in PPV. This hypothesis is further supported by temperature-dependent anisotropy data for PPV (Figure 7a). At 16 K, the anisotropy is constant at a value of about 0.15 on a time scale >100 ps. As the temperature is increased, the anisotropy starts to decay, indicating depolarization likely due to diffusing luminescent excitons. We can see the anisotropy decays to zero at 290 K on the same time scale as the fluorescence decay at 290 K. Experiments by Bazan et al. controlling intermolecular spacing of well-characterized PPV segments also show, at room temperature, this type of lifetime behavior consistent with intermolecular exciton diffusion to defects.[46] At 16 K, measurements for PPV on a time scale <100 ps show a constant anisotropy over the same temperature range ruling out the possibility of unresolved ultrafast exciton diffusion.[25] Examination of the time-dependent PPV spectra show no sign of excimer formation at low (Figure 4a) or high temperatures, as has been observed in MEH−PPV.[24,47] Therefore, our data support the idea of exciton diffusion controlling the fluorescence decay of PPV. It is important to note that although we can freeze out exciton diffusion at lower temperatures, increasing the relative fluorescence yield by a factor of 4, there may be other nonradiative decay channels that lower

the overall fluorescence yield. Rothberg and co-workers have postulated that there is an essentially instantaneous (<100 fs) formation of nonemissive polaron pairs which then slowly recombine, leading to the weak long-lived decays in Figure 6.[37] Such an ultrafast decay channel would not be resolved in our experiment but would provide another mechanism to lower the photoluminescence efficiency.

Turning to the MH−PPV data, we see that the total Stokes shift is considerably enhanced in the neat film as opposed to the dilute blend. It would then appear that roughly 50% of the dynamic Stokes shifting in MH−PPV is due to intermolecular processes, for example, exciton diffusion or excimer formation. It has been established that interchain species play a major role in fluorescence dynamics of MEH−PPV,[48] although the exact nature of all of these species is still a matter of debate. At 16 K, it is clear that the 0−0 vibronic peak in MH−PPVs emission spectrum decays much faster than the 0−1 peak, and we are left with a broad, featureless, red-shifted component after about 2000 ps (Figure 5a). This is also consistent with measurements in MEH−PPV and can be attributed to excimer emission,[24] because its energy is greater than that expected for phosphorescence.[49] The fact that there is no anisotropy decay during this redshift also suggests that excimer formation, rather than exciton diffusion, is responsible for the observed redshift. At higher temperatures, the spectrum broadens and the excimer emission becomes less pronounced.

The temperature-dependent fluorescence decays of MH−PPV shown in Figure 6b do not display the same strong temperature dependence seen in PPV. The 1/e decay times range from 250 to 320 ps, with the lower temperature data the same within experimental error, making it difficult to extract an activation energy. These times are similar to what was observed in MEH−PPV at 77 K, but our fluorescence is longer-lived at room temperature than what was observed by Jakubiak et al.[47] The anisotropy measurements for MH−PPV on the time scale >100 ps show no decay, but the value for the 290 K anisotropy drops to 0.02 from a value of 0.15 for 16 and 100 K. This may indicate some kind of fast exciton movement in MH−PPV at times earlier than 50 ps. Schwartz and co-workers have shown evidence for very fast exciton movement with decaying anisotropies on the time scale <50 ps that our streak camera cannot resolve.[50] It is possible that excimer formation on these time scales is enabled by fast exciton diffusion on this time scale. On the time scale we are observing, however, it is apparent that MH−PPVs dynamics are not dominated by the same picosecond exciton diffusion as in PPV but rather by excimer formation.

The differences described above between PPV and MH−PPV can be explained, in large part, by differences in their intermolecular interactions. PPV has a p2gg unit cell structure that results in a "herringbone" pattern of the phenyl rings when looking down the chain axis of the crystal. The edge-to-face interaction prevents π-orbital overlap and does not favor excimer formation. Studies on model 2,5-substituted oligomers suggest that MH−PPV, on the other hand, stacks with its rings in a face-to-face geometry,[51−53] allowing a large amount of $\pi-\pi$ interaction between molecules. It is the face-to-face geometry that favors excimer formation and explains why we see excimer emission in low-temperature MH−PPV but not in PPV. The same observation was made by Rothberg concerning differences in structure resulting in different species controlling the dynamics in PPV and MH−PPV.[24]

Our work has several implications for the design of electroluminescent materials. Because chain packing determines the species that controls the luminescent dynamics in PPV and its derivatives, control of the chain packing should increase the quantum efficiency of the film. The ideal polymer would have substituents that allow for herringbone packing to prevent excimer formation but also that constrain the rings so that the motions leading to energy transfer (ring torsions) have higher activation energies than in PPV. In alkoxy-substituted PPVs such as MEH−PPV and MH−PPV, this is accomplished through the hydrogen bonding interaction of the ether oxygen with a hydrogen on an adjacent ring, but as described above, this type of substitution also leads to intermolecular interactions that favor excimer formation. It is important to emphasize that crystalline structure in and of itself is not necessarily detrimental to luminescence dynamics, and such regular structure should also enhance the charge transport characteristics of the material. In fact, the first electrically pumped organic lasers are based on highly crystalline tetracene, which crystallizes in the herringbone motif.[54]

V. Conclusion

We have shown that dynamic Stokes shifting in PPV is similar to that observed in an isolated oligomer and is largely due to intramolecular relaxation. Temperature-dependent measurements of the fluorescence decay and anisotropy are consistent with activated exciton diffusion to quenching defects in PPV. Temperature-dependent measurements and time-resolved spectral measurements indicate excimer formation, and not exciton diffusion, dominates the fluorescence dynamics of MH−PPV. In neither case do the wavelength-resolved fluorescence dynamics provide a direct measurement of exciton diffusion in the energy landscape of the polymer. X-ray data on PPV and MH−PPV films provide evidence that the different dynamics in the two conjugated polymers is due to differences in the chain packing which allows greater $\pi-\pi$ interaction in MH−PPV than in unsubstituted PPV.

Acknowledgment. C.J.B. acknowledges support from a 3M Untenured Faculty Award, Dreyfus New Faculty Award, and NSF CAREER Award No. 9984683.

References and Notes

(1) Friend, R. H.; Gymer, R. W.; Holmes, A. B.; Burroughes, J. H.; Marks, R. N.; Taliani, C.; Bradley, D. D. C.; Santos, D. A. D.; Bredas, J. L.; Logdlund, M.; Salaneck, W. R. *Nature* **1999**, *397*, 121−128.

(2) Woo, H. S.; Lhost, O.; Graham, S. C.; Bradley, D. D. C.; Friend, R. H.; Quattrocchi, C.; Bredas, J. L.; Schenk, R.; Mullen, K. *Synth. Met.* **1993**, *59*, 13−28.

(3) Hayes, G. R.; Samuel, I. D. W.; Phillips, R. T. *Phys. Rev. B* **1995**, *52*, 11569−11572.

(4) Kersting, R.; Mollay, B.; Rusch, M.; Wenisch, J.; Leising, G.; Kauffmann, H. F. *J. Chem. Phys.* **1997**, *106*, 2850−2864.

(5) Bassler, H.; Schweitzer, B. *Acc. Chem. Res.* **1999**, *32*, 173−182.

(6) Hayes, G. R.; Samuel, I. D. W.; Phillips, R. T. *Phys. Rev. B* **1997**, *56*, 3838−3843.

(7) Credo, G. M.; Lowman, G. M.; DeAro, J. A.; Carlson, P. J.; Winn, D. L.; Buratto, S. K. *J. Chem. Phys.* **2000**, *112*, 7864−7872.

(8) Adams, D. M.; Kerimo, J.; O'Connor, D. B.; Barbara, P. F. *J. Phys. Chem. A* **1999**, *103*, 10138−10143.

(9) Yu, J.; Hu, D. H.; Barbara, P. F. *Science* **2000**, *289*, 1327−1330.

(10) Burn, P. L.; Bradley, D. D. C.; Brown, A. R.; Friend, R. H.; Holmes, A. B. *Synth. Met.* **1991**, *41−43*, 261−264.

(11) Burn, P. L.; Bradley, D. D. C.; Friend, R. H.; Halliday, D. A.; Holmes, A. B.; Jackson, R. W.; Kraft, A. *J. Chem. Soc., Perkin Trans. 1* **1992**, 3225−3231.

(12) Gagnon, D. R.; Capistran, J. D.; Karasz, F. E.; Lenz, R. W.; Antouns, S. *Polymer* **1987**, *28*, 567−573.

(13) Stenger-Smith, J. D.; Lenz, R. W.; Wegner, G. *Polymer* **1989**, *30*, 1048−1053.

(14) Bjorklund, T. G.; Lim, S.-H.; Bardeen, C. J. *Synth. Met.* In press.

(15) Shah, H. V.; Arbuckle, G. A. *Macromolecules* **1999**, *32*, 1413−1423.
(16) Burn, P. L.; Kraft, A.; Baigent, D. R.; Bradley, D. D. C.; Brown, A. R.; Friend, R. H.; Gymer, R. W.; Holmes, A. B.; Jackson, R. W. *J. Am. Chem. Soc.* **1993**, *115*, 10117−10124.
(17) Schenk, R.; Gregorius, H.; Meerholz, K.; Heinze, J.; Müllen, K. *J. Am. Chem. Soc.* **1991**, *113*, 2634−2647.
(18) Klug, H. P.; Alexander, L. E. *X-ray Diffraction Procedures For Polycrystalline and Amorphous Materials*; John Wiley & Sons: New York, 1954.
(19) Willhelm, T.; Piel, J.; Riedle, E. *Opt. Lett.* **1997**, *22*, 1494−1496.
(20) Krylov, V.; Gallus, J.; Wild, U. P.; Kalintsev, A.; Rebane, A. *Appl. Phys. B* **2000**, *70*, 163−168.
(21) Denton, G. J.; Tessler, N.; Stevens, M. A.; Friend, R. H. *Adv. Mater.* **1997**, *9*, 547−551.
(22) Tessler, N.; Denton, G. J.; Harrison, N. T.; Stevens, M. A.; Burns, S. E.; Friend, R. H. *Synth. Met.* **1997**, *91*, 61−64.
(23) Pichler, K.; Halliday, D. A.; Bradley, D. D. C.; Burn, P. L.; Friend, R. H.; Holmes, A. B. *J. Phys. Condens. Matter* **1993**, *5*, 7155−7172.
(24) Jakubiak, R.; Yan, M.; Wan, W. C.; Hsieh, B. R.; Roghtberg, L. J. *Israel J. Chem.* **2000**, *40*, 153−157.
(25) Lim, S.-H.; Bjorklund, T. G.; Bardeen, C. J. *Chem. Phys. Lett.* **2001**, *342*, 555−562.
(26) Yu, J.; Hayashi, M.; Lin, S. H.; Liang, K. K.; Hsu, J. H.; Fann, W. S.; Chao, C.; Chuang, K.; Chen, S. *Synth. Met.* **1996**, *82*, 159−166.
(27) Bradley, D. D. C. *J. Phys. D: Appl. Phys.* **1987**, *20*, 1389−1410.
(28) Chen, D.; Winokur, M. J.; Masse, M. A.; Karasz, F. E. *Polymer* **1992**, *33*, 3116−3122.
(29) Lovinger, A. J.; Rothberg, L. J. *J. Mater. Res.* **1996**, *11*, 1581−1592.
(30) Silinsh, E. A.; Capek, V. *Organic Molecular Crystals*; A. I. P. Press: Woodbury, NY, 1994.
(31) Masse, M. A.; Martin, D. C.; Thomas, E. L.; Karasz, F. E.; Petermann, J. H. *J. Mater. Sci.* **1990**, *25*, 311−320.
(32) Balagurov, B. Y.; Vaks, V. G. *Sov. Phys.-JETP* **1974**, *38*, 968−971.
(33) Hess, B. C.; Kanner, G. S.; Vardeny, Z. V.; Baker, G. L. *Phys. Rev. Lett.* **1991**, *66*, 2364−3267.
(34) Kanner, G. S.; Wei, X.; Hess, B. C.; Chen, L. R.; Vardeny, Z. V. *Phys. Rev. Lett.* **1992**, *69*, 538−541.
(35) Nguyen, T.; Doan, V.; Schwartz, B. J. *J. Chem. Phys.* **1999**, *110*, 4068−4078.
(36) Powell, R. C.; Soos, Z. G. *J. Lumin.* **1975**, *11*, 1−45.
(37) Rothberg, L. J.; Yan, M.; Papadimitrakopoulos, F.; Galvin, M. E.; Kwock, E. W.; Miller, T. M. *Synth. Met.* **1996**, *80*, 41−58.
(38) Yan, M.; Rothberg, L. J.; Kwock, E. W.; Miller, T. M. *Phys. Rev. Lett.* **1995**, *75*, 1992−1995.
(39) Powell, R. C.; Kepler, R. G. *Phys. Stat. Sol. B* **1973**, *55*, K89.
(40) Greenham, N. C.; Samuel, I. D. W.; Hayes, G. R.; Phillips, R. T.; Kessener, Y. A. R. R.; Moratti, S. C.; Holmes, A. B.; Friend, R. H. *Chem. Phys. Lett.* **1995**, *241*, 89−96.
(41) Yan, M.; Rothberg, L. J.; Papadimitrakopoulos, F.; Galvin, M. E.; Miller, T. M. *Phys. Rev. Lett.* **1994**, *73*, 744−747.
(42) Heller, C. M.; Campbell, I. H.; Laurich, B. K.; Smith, D. L.; Bradley, D. D. C.; Burn, P. L.; Ferraris, J. P.; Mullen, K. *Phys. Rev. B* **1996**, *54*, 5516−5522.
(43) Mao, G.; Fischer, J. E.; Karasz, F. E.; Winokur, M. J. *J. Chem. Phys.* **1993**, *98*, 712−716.
(44) Sluch, M. I.; Godt, A.; Bunz, U. H. F.; Berg, M. A. *J. Am. Chem. Soc.* **2001**, in press.
(45) Brunner, K.; Tortschanoff, A.; Warmuth, C.; Bassler, H.; Kauffmann, H. F. *J. Phys. Chem. B* **2000**, *104*, 3781−3790.
(46) Bazan, G. C.; Miao, Y.-J.; Renak, M. L.; Sun, B. J. *J. Am. Chem. Soc.* **1996**, *118*, 2618−2624.
(47) Jakubiak, R.; Collison, C. J.; Wan, W. C.; Rothberg, L. J.; Hsieh, B. *J. Phys. Chem. A* **1999**, *103*, 2394−2398.
(48) Nguyen, T.; Martini, I. B.; Liu, J.; Schwartz, B. J. *J. Phys. Chem. B* **2000**, *104*, 237−255.
(49) Monkman, A. P.; Burrows, H. D.; Miguel, M. d. G.; Hamblett, I.; Navaratnam, S. *Chem. Phys. Lett.* **1999**, *307*, 303−309.
(50) Nguyen, T.; Wu, J.; Doan, V.; Schwartz, B. J.; Tolbert, S. H. *Nature* **2000**, *288*, 652−656.
(51) Hutten, P. F. v.; Wildeman, J.; Meetsma, A.; Hadziioannou, G. *J. Am. Chem. Soc.* **1999**, *121*, 5910−5918.
(52) Resel, R.; Kiebooms, R.; Vanderzande, D.; Stelzer, F. *Monatsh. Chem.* **2001**, *132*, 433−440.
(53) Stalmach, U.; Schollmeyer, D.; Meier, H. *Chem. Mater.* **1999**, *11*, 2103-2106.
(54) Schon, J. H.; Kloc, C.; Dodabalapur, A.; Batlogg, B. *Science* **2000**, *289*, 599−601.